The Effect of Cholesterol on the Lateral Diffusion of Phospholipids in Oriented Bilayers

Andrey Filippov, Greger Orädd, and Göran Lindblom
Department of Biophysical Chemistry, Umeå University, SE-90187 Umeå, Sweden

ABSTRACT   Pulsed field gradient NMR was utilized to directly determine the lipid lateral diffusion coefficient for the following macroscopically aligned bilayers: dimyristoylphosphatidylcholine (DMPC), sphingomyelin (SM), palmitoyloleoylphosphatidyl-choline (POPC), and dioleoylphosphatidylcholine (DOPC) with addition of cholesterol (CHOL) up to ~40 mol %. The observed effect of cholesterol on the lipid lateral diffusion is interpreted in terms of the different diffusion coefficients obtained in the liquid ordered (l_o) and the liquid disordered (l_d) phases occurring in the phase diagrams. Generally, the lipid lateral diffusion coefficient decreases linearly with increasing CHOL concentration in the l_d phase for the PC-systems, while it is almost independent of CHOL for the SM-system. In this region the temperature dependence of the diffusion was always of the Arrhenius type with apparent activation energies (E_A) in the range of 28–40 kJ/mol. The l_o phase was characterized by smaller diffusion coefficients and weak or no dependence on the CHOL content. The E_A for this phase was significantly larger (55–65 kJ/mol) than for the l_d phase. The diffusion coefficients in the two-phase regions were compatible with a fast exchange between the l_d and l_o regions in the bilayer on the timescale of the NMR experiment (100ms). Thus, strong evidence has been obtained that fluid domains (with size of μm or less) with high molecular ordering are formed within a single lipid bilayer. These domains may play an important role for proteins involved in membrane functioning frequently discussed in the recent literature. The phase diagrams obtained from the analysis of the diffusion data are in qualitative agreement with earlier published ones for the SM/CHOL and DMPC/CHOL systems. For the DOPC/CHOL and the POPC/CHOL systems no two-phase behavior were observed, and the obtained E_A:s indicate that these systems are in the l_d phase at all CHOL contents for temperatures above 25°C.

INTRODUCTION

There are an extraordinary number of investigations of cholesterol in lipid membranes, studies that started at least 70 years ago. Surprisingly, a comprehensive understanding of the functioning of cholesterol in membranes at the molecular level has still not been reached. In most of these investigations the lipid component is phosphatidylcholines (PCs), mainly dipalmitoyl-PC (DPPC), i.e., a lipid with saturated acyl chains. One of the unique physicochemical properties of cholesterol, namely the so-called condensing effect, observed in monolayers at a water-air interface was reported already 1925 (Leathes, 1925). Another important property of cholesterol was shown by differential scanning calorimetry (DSC). Cholesterol at sufficiently high concentrations was found to eliminate the phase transition (the so-called main transition) between a gel with crystalline acyl chains and the liquid crystalline phase of phospholipids (De Kruijff et al., 1973; Ipsen et al., 1987; Ulmius et al., 1975; Yeagle, 1985). Later it was shown by ^{2}H-NMR spectroscopy that the presence of cholesterol in a liquid crystalline phase of a lipid bilayer drastically increased the molecular ordering of the acyl chains (Haberkorn et al., 1977; Oldfield et al., 1978; Stockton and Smith, 1976). On the other hand, addition of cholesterol to the gel phase results in a decrease in the order parameter of the chains. It has also been shown that the lipid membrane permeability is decreased by cholesterol (Fiorini

et al., 1989) and that the bilayer thickness increases (McIntosh, 1978). The first detailed phase diagram of the ternary system DPPC, cholesterol, and water was reported as late as 1990 and was determined with ^{2}H-NMR spectroscopy and calorimetry (Vist and Davis, 1990). The most striking property of this phase diagram is the existence of a two-phase region flanked by one-phase areas, one at low cholesterol content, the liquid disordered phase (l_d), and one at high cholesterol content, the liquid ordered phase (l_o). While both the l_d and l_o phases exhibit the fast rotational and translational motion characteristic for a liquid crystalline phase, the acyl chains of the l_o phase are highly ordered (Vist and Davis, 1990). In a theoretical investigation the whole phase diagram was reproduced (Ipsen et al., 1987), and the characteristics of the phase diagram have been suggested to be quite similar for phospholipids containing one mono-unsaturated acyl chain (Thewalt and Bloom, 1992). Unfortunately, no such detailed investigation has been reported for sphingolipids (SM), another class of important membrane lipids. These lipids often coexist with cholesterol at high concentrations, and only some scattered studies have been published so far (Guo et al., 2002; Maulik and Shipley, 1996a,b; Sankaram and Thompson, 1990; Smaby et al., 1994). In recent years another property of cholesterol has been suggested from a large number of studies, namely that cholesterol might induce domains in lipid bilayers composed of PCs or SMs having saturated acyl chains (Brown, 1998; Rietveld and Simons, 1998; Samsonov et al., 2001; Simons and Ikonen, 1997). Such domains, often called ''rafts'', were not obtained with unsaturated lipids. McConnell and co-workers have taken a different approach and they have

published several studies on monolayers, where aggregation between cholesterol and saturated PCs or SMs appears, called ''condensed complexes'' (Radhakrishnan et al., 2001; Radhakrishnan and McConnell, 1999). Recently, the latter model from monolayers was applied to DSC data from saturated phospholipid/cholesterol systems (Anderson and McConnell, 2001). The DSC curve could be reproduced, and, furthermore, it was suggested that the broad heat absorption experimentally observed is due to the thermal dissociation of the condensed complexes.

The molecular mobility is another important aspect of lipids in biomembranes. ^{2}H-NMR relaxation measurements suggest that axial rotational diffusion of phospholipid molecules occurs at a somewhat higher rate when cholesterol is present in the lipid membrane than in a bilayer of a single lipid as a consequence of the high ordering and reduction in chain entanglements (Trouard et al., 1999; Weisz et al., 1992). Effects of cholesterol on the translational mobility of lipids have been reported in a number of works (Almeida et al., 1992; Kuo and Wade, 1979; Ladha et al., 1996; Lindblom et al., 1981; Orädd et al., 2002). The most extensive study in the last decade is that of Almeida et al. (1992), who made a systematic study using the fluorescence recovery after photobleaching (FRAP) technique of the temperature and concentration dependences of the averaged lipid diffusion coefficient in dimyristoyl-PC (DMPC)-cholesterol systems. The results obtained for lipids having unsaturated acyl chains show that the presence of cholesterol in fluid bilayers can result in an increase in the diffusion coefficient (Ladha et al., 1996; Lindblom et al., 1981). Generally, simulation studies are in accordance with the results of experimental investigations (Chiu et al., 1999; Polson et al., 2001; Smondyrev and Berkowitz, 1999).

The aim of the present work is to determine the effect of cholesterol on the lipid lateral self-diffusion in bilayers containing PCs or SMs and to see if cholesterol/lipid domains or complexes can be detected on the time-scale of the NMR diffusion experiment.

MATERIALS AND METHODS

Materials

The compounds used for the preparation of macroscopically aligned bilayers were:

1,2-dioleoyl-sn-glycero-3-phosphocholine (DOPC), 1-palmitoyl-2-oleoyl-sn-glycero-3-phosphocholine (POPC), 1,2-dimyristoyl-sn-glycero-3-phosphocholine (DMPC), chicken egg yolk sphingomyelin (SM), and 5-cholesten-3β-ol (CHOL). DOPC, POPC and DMPC were from Avanti Polar Lipids (Birmingham, AL), while SM and CHOL were from Sigma (St. Louis, MO). Deuterated water (^{2}H$_2$O, 99.7%) was purchased from Larodan AB (Malmö, Sweden).

Sample preparation

Binary mixtures of lipid and sterol were prepared by dissolving the lipid and CHOL in a mixture of methanol and propanol (1:4 vol) at a concentration of

15 mg/ml. A total of 25 μl of the solution was put onto each of 60 glass plates (5 × 14 mm^2). The solvent was evaporated at atmospheric pressure and then under vacuum at 30°C for 6 h. The glass plates were stacked and placed in a humid ^{2}H$_2$O atmosphere in order to form hydrated bilayers, and the amount of water was then adjusted to obtain 35 wt % (DMPC and SM) or 30 wt % (DOPC and POPC). Crossed polaroids were used to check the orientation of the hydrated bilayers.

pfg-NMR

^{1}H pulsed field gradient (pfg) NMR diffusion measurements were performed at 100 MHz using a Varian/Chemagnetics CMX Infinity spectrometer, equipped with a purpose-built goniometer probe (Cryomagnet systems, Indianapolis, IN). By rotating the stack of glass plates the bilayer normal can be oriented at the so-called magic angle of 54.7° with respect to the main magnetic field. This causes the dipolar interactions to vanish with a significant reduction of the line widths as a result (Lindblom and Orädd, 1994). For the used stimulated echo pulse sequence (Fig. 1) the diffusion decay (DD) of the echo amplitude A can be described by the equation (Tanner, 1970):

$$A = \frac{I}{2} \cdot \exp\left(\frac{-2\tau}{T_2}\right) \cdot \exp\left(\frac{\tau_1}{T_1}\right)$$
$$\cdot \exp\left(-\gamma^2 \cdot \delta^2 \cdot g^2 \cdot D \cdot \left(\Delta - \frac{\delta}{3}\right)\right), \qquad (1)$$

where the initial echo amplitude (without the magnetic field gradient) is determined by the longitudinal and transverse NMR relaxation times (T_1 and T_2), and I is a factor proportional to the proton content in the system. In the last exponent, which determines the decay due to diffusion, γ is the gyromagnetic ratio; Δ is the time interval between the two gradient pulses; ($\Delta - \delta/3$) is the diffusion time; δ and g are the duration and amplitude of the pulsed field gradients, respectively; and D is the self-diffusion coefficient.

In our experiments $g = 1.15\ T$/m was set constant and δ was varied in the range of 0.3–9 ms in 10 to 32 steps while all the other variables were held constant. The range of values for τ and τ_1 used in these experiments were 4.5–11 and 50–250 ms, respectively. The resulting D values did not depend on these parameters, and the majority of the experiments were performed with $\tau = 11$ ms and $\tau_1 = 100$ ms. Signal accumulations from 16 to 320 were made to obtain acceptable signal-to-noise levels. Experimental echoes were Fourier transformed into corresponding sets of spectra, and a nonlinear fit of the obtained signal decay then gives the diffusion coefficient, D. The observed results were not dependent on the chosen value of Δ in the range of 60–160 ms.

In Eq. 1 it is assumed that the effect of background field gradients is negligible and that the diffusion motion can be described by a single component. If the signal amplitude contains contributions from more than one species or if there is a slow exchange between different motional sites, the decay will be a sum of exponents instead of a single one. If the exchange is fast compared with the diffusion time, a single diffusion coefficient will again be observed, with the value of D determined as the average of the
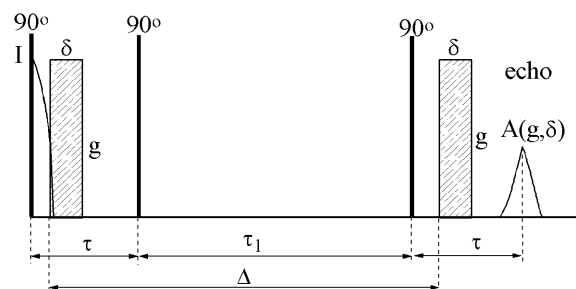

FIGURE 1 A schematic of the stimulated echo pulse sequence used in this work. RF pulses are shown as filled rectangles, whereas the gradient pulses are hatched. The NMR signal is acquired from the top of the echo.

separate diffusion coefficients, weighted by the respective populations of the sites. Moreover, Eq. 1 is valid only as long as the diffusion is unrestricted, a condition that can be written as $a = D \cdot \Delta/R^2 \ll 1$, where R is the distance between restrictions in the direction of the pulsed gradient. If this condition is not fulfilled, the DD changes and the apparent self-diffusion coefficient (D_{app}) will become dependent on Δ. The precise Δ-dependence of the DD and D_{app} is determined by the size and geometry of the restrictions (Callaghan, 1991; Kärger et al., 1988).

RESULTS

^{1}H-NMR spectra

NMR spectra of lamellar phases of POPC, DOPC, and SM, oriented at the magic angle, along with reference solution spectra of DOPC and SM are illustrated in Fig. 2. For oriented bilayers of POPC, DOPC, and SM, the NMR peaks are broad (Fig. 2, A–C) in comparison with the solution spectra (Fig. 2, D and E) but the main peaks, corresponding to the hydrocarbon chains, $(CH_2)_n$, and the choline head-group, $(CH_3)_3$, are still clearly resolved. The shapes of the NMR spectra in Fig. 2, A–C do not depend on the applied gradient strength, but the relative signal amplitudes of the different peaks depend on the time intervals τ and τ_1 of the stimulated echo pulse sequence. The shape of the SM and DMPC spectra also changes with temperature, in particular when passing T_m, equal to 313 K for SM and 297 K for DMPC.

For POPC and DOPC (Fig. 2, A and B) the relative peak intensities correspond well to the integral intensities of the peaks of the solution spectra, while for SM (Fig. 2 C) the CH_2 and CH_3 peaks of the hydrocarbon chains are diminished relative to the headgroup $(CH_3)_3$ signal. This is indicative of an increased relaxation of the chain protons compared to the headgroup protons. The presence of CHOL produced no additional lin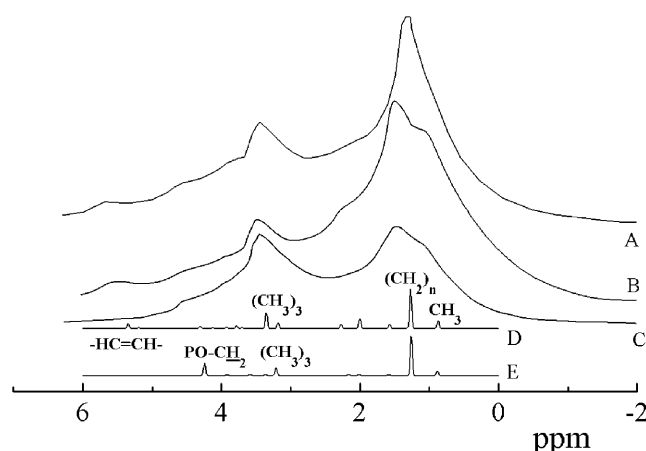es in the spectra of the liquid crystalline phase, probably due to the fast relaxation in this rather rigid molecule. However, the spectra of all lipids are dependent on the CHOL content.

The NMR diffusion decay

Due to the severe overlap of signals for this instrumentation, the whole NMR spectrum was integrated and this value was used in the fit. This means that the DD will contain contributions from both the water signal and the lipid signals. Fig. 3 presents a typical DD. It can be described as the sum of two components:

$$A(k) = P_1 \cdot \exp(-k \cdot D_1 \cdot (\Delta - \delta/3)) + P_2 \cdot \exp(-k \cdot D_2 \cdot (\Delta - \delta/3)), \quad (2)$$

where $k = (\gamma g \delta)^2$ and P_1 and P_2 are the apparent populations of protons. The fast decay gives a D_1 of $\sim 10^{-10}$ m^2/s, which is typical for water between bilayers (Lindblom and Orädd, 1994; Wassall, 1996). This component, originating from water, was not further analyzed in the present study. The second component of the DD arises from the lipids. This is clear from the obtained D_2, with a magnitude typical for lipids (10^{-12} m^2/s–10^{-11} m^2/s) (Lindblom and Orädd, 1994), and also from the chemical shifts of the slowly diffusing component generally observed for lipids (see Fig. 2). This part of the DD was always exponential and thus gives the lipid lateral diffusion coefficient, D_L, after multiplying D_2 by the factor 1.5. It is assumed that the lipid diffusion occurs in the plane of the bilayers only, i. e., no lipid diffusion occurs perpendicular to the membrane (Lindblom and Orädd, 1994; Wästerby et al., 2002).

Diffusion in lipid/cholesterol bilayers

Fig. 4 summarizes the results obtained for the SM/CHOL system. Fig. 4 A presents the phase diagram determined by Sankaram and Thompson (1990). Part of the phase diagram is characterized by an extensive two-phase area with the l_d

FIGURE 2 ^{1}H-NMR spectra of POPC (A), DOPC (B), and SM (C) in oriented bilayers with 20 wt % ^{2}H$_2$O obtained from the pfg-NMR stimulated echo after suppression of the signal from the residual water protons. $T = 333$ K. Parameters of the stimulated echo pulse sequence are $\delta = 1.5$ ms, $\tau = 11$ ms, and $\tau_1 = 100$ ms. Solution ^{1}H-NMR spectra of DOPC (D) and SM (E) are shown below for reference.
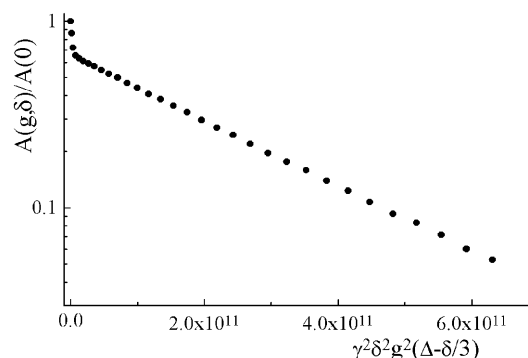

FIGURE 3 Diffusion decay of an oriented POPC bilayer with 30 wt % ^{2}H$_2$O at 303 K and a diffusion time of 100 ms. The early, fast decay is attributed to water diffusion, whereas the latter, slow decay corresponds to the lipid diffusion.
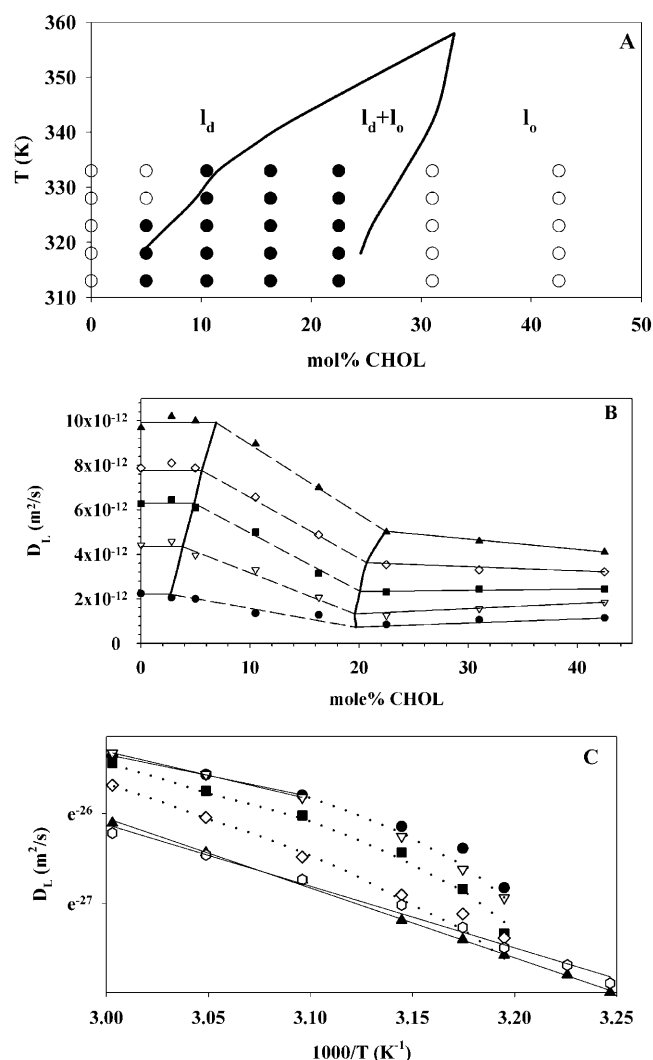
D_L is largely independent of CHOL content and D_L seems even to increase a little by a small CHOL addition, but the quality of the data prevents any firm conclusion on this. At intermediate CHOL contents, from ~5 to 20 mol %, D_L decreases sharply and then levels off to an almost constant value at the highest CHOL contents. The temperature dependence is shown in Fig. 4 C. At CHOL concentrations above 20 mol % the curves are approximately linear with apparent activation energies of 55–65 kJ/mol. The curves for lower CHOL contents are nonlinear, especially close to $T_m = 313$ K of the lipid. For the 0 and 5 mol % CHOL contents, a linear dependence is indicated by straight lines for the three highest temperatures. The obtained apparent activation energies (E_A) from the straight lines in Fig. 4 C are listed in Table 1.

A corresponding study for the DMPC/CHOL system is summarized in Fig. 5. The phase borders in Fig. 5 A are taken from Sankaram and Thompson (1990) and Almeida et al. (1992). The lateral diffusion in the DMPC/CHOL system is characterized by a slow linear dependence of D_L on the CHOL concentration (Fig. 5 B). At the highest CHOL concentrations the diffusion is nearly constant, and lowering the temperature extends the area of constant D_L to lower CHOL content. The reciprocal temperature dependence is found to be linear (Arrhenius) for high and low additions of CHOL, while the dependence at intermediate CHOL concentrations is clearly nonlinear (Fig. 5 C). The calculated E_A values from the straight lines in Fig. 5 C are given in Table 1.

FIGURE 4 (*A*) Phase diagram of the SM/CHOL system according to Sankaram and Thompson (1990). The circles mark experimental points investigated by us. Open and filled circles correspond to samples from one-phase and two-phase regions, respectively. (*B*) Lateral diffusion coefficients at different CHOL concentrations for the SM/CHOL system with 35 wt % ^2H_2O and at 313 K (*circle*), 318 K (*triangle top down*), 323 K (*square*), 328 K (*diamond*), and 333 K (*triangle top up*). The thick solid lines are estimations of the extension of the two-phase area. The solid and dotted lines are linear estimations of D_L in the one-phase and two-phase areas, respectively. (*C*) Arrhenius plots of the temperature dependence of the lateral diffusion coefficient for the SM/CHOL system with 35 wt % ^2H_2O and CHOL contents varying as 0 (*circles*), 5 (*triangle top down*), 10.5 (*square*), 16.3 (*diamond*), 31 (*triangle top up*), and 42.5 mol % (*hexagon*). The solid lines are Arrhenius fits to the data in the one-phase regions, whereas the dotted lines are the calculated D_L according to the lever rule in the two-phase area. In these calculations the phase borders obtained by us have been used (*thick lines* in Fig. 4 B).

TABLE 1   Apparent activation energies obtained in the one-phase areas of the investigated systems in the temperature range of 298–333 K

System	Mol % CHOL	Phase	E_A (kJ/mol)
SM/CHOL (Fig. 4 *C*)	0	l_d	39*
	5	l_d	44*
	31	l_o	64
	42.5	l_o	57
DMPC/CHOL (Fig. 5 *C*)	0	l_d	31[†]
	5	l_d	36[†]
	15	l_d	37
	35	l_o	55
DOPC/CHOL (Fig. 6 *A*)	0	l_d	27
	5.1	l_d	28
	9.5	l_d	29
	14.5	l_d	31
	25	l_d	31
	33.5	l_d	32
	46.5	l_d	32
POPC/CHOL (Fig. 6 *B*)	0	l_d	28
	6.6	l_d	29
	12	l_d	29
	22.5	l_d	31
	33.7	l_d	33
	48.8	l_d	37

The E_A values correspond to the straight lines in Figs. 4 C and 5 C and 6, A and B.
*313 ≤ T ≤ 333 K.
[†]$T = 298$ K excluded.

and l_o phases extending from 5 to 30 mol % CHOL and from 310 to ~360 K. In this figure our measured points are marked with open circles corresponding to points classified to be one-phase areas and filled circles belonging to two-phase regions. Fig. 4 B shows the obtained D_L as a function of CHOL content. At the lowest concentrations of CHOL,
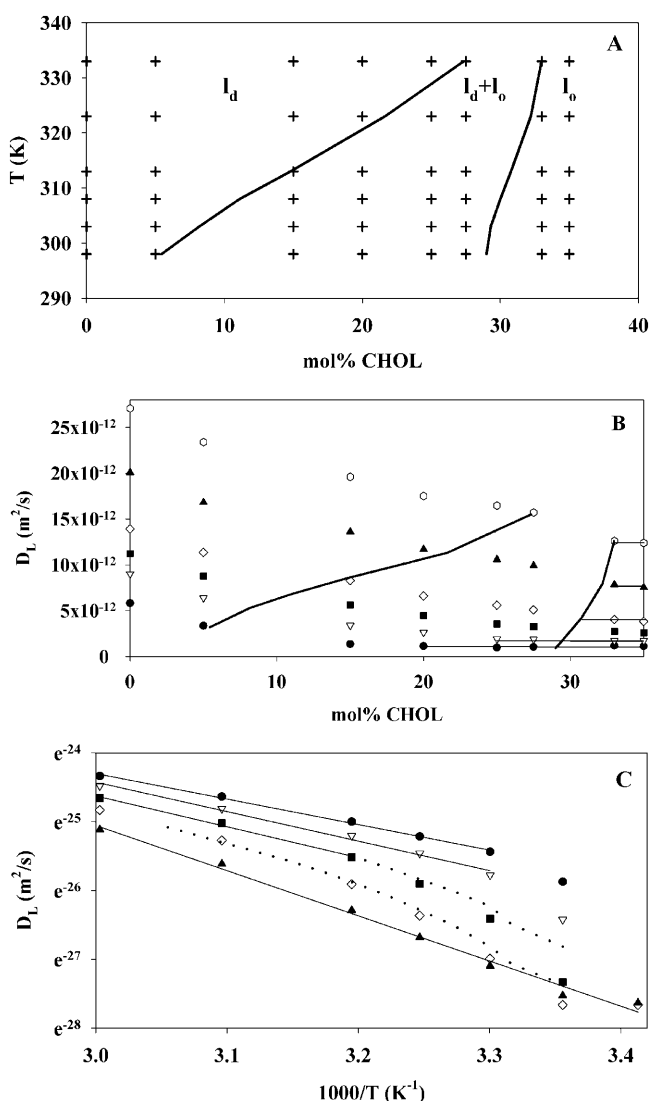
FIGURE 5 (*A*) Phase diagram of the DMPC/CHOL system according to Almeida et al. (1992). The crosses mark experimental points investigated by us. (*B*) Lipid lateral diffusion coefficients at different CHOL concentrations for the DMPC/CHOL system with 35 wt % ^{2}H$_2$O and at 298 K (*circle*), 303 K (*triangle top down*), 308 K (*square*), 313 K (*diamond*), 323 K (*triangle top up*), and 333 K (*hexagon*). The solid lines are drawn through the concentrations for which D_L is approximately constant. These points are tentatively assigned to the l_o one-phase area. (*C*) Arrhenius plots of the temperature dependence of the lipid lateral diffusion coefficient for the DMPC/CHOL system with 35 wt % ^{2}H$_2$O and varying CHOL contents of 0 (*circles*), 5 (*triangle top down*), 15 (*square*), 25 (*diamond*), and 35 mol % (*triangle top up*). The solid lines are Arrhenius fits to the data in the one-phase regions, whereas the dotted lines are the calculated D_L according to the lever rule in the two-phase area. In these calculations the phase borders given by Almeida et al. (1992) have been used (*thick lines* in Fig. 5, *A* and *B*).

Fig. 6 shows the concentration dependence of D_L for the DOPC/CHOL (*A*) and POPC/CHOL (*B*) systems. D_L decreases linearly with CHOL content in both systems. The reciprocal temperature dependence in these systems is found to be linear with apparent activation energies for the diffusion process ranging between 27–32 kJ/mol for the DOPC system
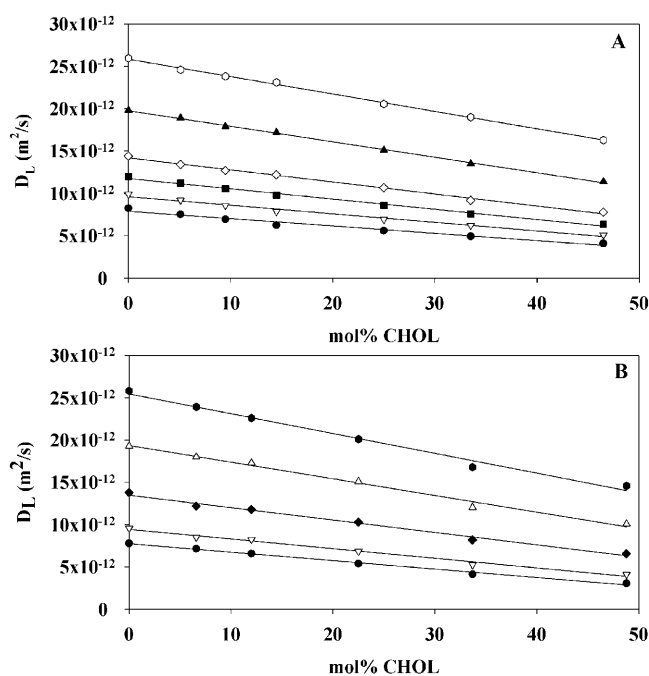

FIGURE 6 Concentration dependences of lipid lateral diffusion coefficients in oriented bilayers of the DOPC/CHOL system (*A*) and the POPC/CHOL system (*B*) with 30 wt % ^{2}H$_2$O and at 298 K (*circles*), 303 K (*triangle top down*), 308 K (*square*), 313 K (*diamond*), 323 K (*triangle top up*), and 333 K (*hexagon*).

and between 28–37 kJ/mol for the POPC system. In general, the activation energies increase monotonically with increasing CHOL content (Table 1).

DISCUSSION

In all measurements D_L is independent of the diffusion time Δ. Therefore, it can be concluded that the lipid motion is unrestricted and, consequently, that D_L is a true molecular self-diffusion coefficient. The fact that D_L is always single exponential is typical for a system with only one diffusion coefficient or, in the case of a system characterized by two or more diffusion coefficients, that there is fast chemical exchange present between the different motional sites. In the case of fast exchange, only an averaged lateral diffusion coefficient is obtained.

The SM/CHOL system

From our data of the SM/CHOL system, one can distinguish three regions with different dependencies of the lateral diffusion coefficient on the temperature (Fig. 4 *C*) and CHOL content (Fig. 4 *B*). These regions can be associated with the l_d and l_o phase areas and the two-phase region between them according to Fig. 4 *A*.

D_L seems to be independent of the CHOL content in the l_d region. It is, however, difficult to draw any firm conclusion, since the l_d region is rather narrow, and the number of

measurements is small. There is some indication that D_L increases slightly at small additions of CHOL. This could possibly reflect the reported ''softening'' of the membranes (Lemmich et al., 1997) and the increased rotational and translational molecular mobility suggested from deuterium relaxation studies (Trouard et al., 1999) for CHOL contents of up to 2–3 mol %. The increase in D_L at low CHOL additions has also been observed at lower water contents, and this is currently under investigation.

In the l_o phase D_L is almost 50% lower than in the l_d phase and it is varying very weakly with the CHOL content. In this phase D_L decreases with CHOL content at temperatures above 323 K, but at lower temperatures D_L increases slightly upon addition of CHOL. This behavior has also been observed in other systems (Almeida et al., 1992) as well as in simulation studies of lipid-sterol systems (Polson et al., 2001).

The region where D_L decreases more steeply coincides well with the two-phase regions of the phase diagram for SM/CHOL and, therefore, we conclude that this decrease in D_L is an effect of the increasing fraction of the l_o phase in the lipid bilayer. Under the assumption of fast exchange the observed D_L in the two-phase area will be an average of the diffusion coefficients at the phase borders to the single-phase areas, i.e., we should obtain a linear dependence of D_L on CHOL concentration in this region. The dotted lines in Fig. 4 B indicates the best fit through the experimental points in the two-phase region of the SM/CHOL system. The phase borders can then be obtained from the crossings of these lines with the lines connecting the points within each of the one-phase areas (for simplicity, a linear dependence is assumed also in the one-phase areas). The phase borders obtained by this procedure are drawn as thick lines in Fig. 4 B, and they are found to shift toward a slightly lower CHOL content, than those in the phase diagram reported by Sankaram and Thompson (1990) (Fig. 4 A).

Fig. 4 C shows that the temperature dependence is mostly non-Arrhenius, even for the pure SM system, except at the highest temperatures. This is probably a consequence of the broad-phase transition observed for SM. Being a compound obtained from biological materials, the composition cannot be expected to be as homogeneous as for synthetically produced molecules and, therefore, the main-phase transition is extended over a large temperature interval. The observed curvature in the Arrhenius plot for pure SM bilayers close to T_m can be explained by the presence of small amounts of lipids in a gel state in the bilayer even at temperatures well above the reported T_m. The temperature dependence of the diffusion coefficient in the l_d phase is obscured by this broad-phase transition and it is, therefore, difficult to draw any firm conclusions in this part of Fig. 4 C. It can be noted that for the highest temperatures, where the dependence is close to Arrhenius, the apparent activation energies of D_L in lipid bilayers with 0 and 5 mol % CHOL are ~40 kJ/mol (Table 1), which compares well with the values obtained for the other investigated systems in the l_d phase. For the l_o phase

the apparent activation energies are significantly higher (Table 1). By applying the lever rule to the points in the two-phase area in Fig. 4 A it is possible to estimate the fractions of lipids in the l_d and l_o phases. These values can be used together with the D_L values for the l_d and l_o phases, obtained at the phase borders in Fig. 4 B to calculate the temperature dependence in the two-phase region. The dotted lines in Fig. 4 C are the results of such calculations. The experimentally obtained values are in good agreement with these lines.

The DMPC/CHOL system

For the DMPC/CHOL system, D_L depends linearly on the CHOL content in the l_d phase, and there is no distinct transition upon the entry into the two-phase region. Obviously, it is not possible to estimate the phase border in the same way as for the SM/CHOL system. However, as for the SM/CHOL system, D_L seems to have a very weak CHOL dependence in the l_o phase. From the region of constant D_L (*solid horizontal lines* in Fig. 5 B) one can estimate the transition into the l_o phase, and this estimation is in good agreement with the phase diagram of Almeida et al. (1992) except at (cf. Fig. 5, A and B) lower temperatures where our data suggest that the two-phase region is more narrow than that obtained by these authors.

The linear dependence of D_L on CHOL content is in contrast with the results obtained by FRAP (Almeida et al., 1992), where D_L was found to be independent of CHOL content in the l_d phase. As a consequence of this difference, our values of D_L for pure DMPC are ~50% higher than those reported by the FRAP method (Almeida et al., 1992; Vaz et al., 1985). The reason for this discrepancy is not clear, but one explanation can be that different timescales are utilized by the two methods in the measurements of the diffusion coefficients. The FRAP method relies on the repopulation of unbleached probes into the bleached spot on the timescale of several seconds and therefore relates to motions over several micrometers in a rim around the bleached spot. On the other hand, pfg-NMR measures translation diffusion on the millisecond timescale, corresponding to distances around one micrometer. FRAP would be expected to be more sensitive than pfg-NMR to cracks or linear defects between different microdomains on the micrometer scale, which would slow down the diffusive motion. It is interesting to note that our values are in good agreement with those of Almeida et al. (1992) in the two-phase region, indicating that the morphology of the bilayers changes toward more homogeneous macroscopic regions in the two-phase area. Another possibility for the large difference in D_L for pure DMPC might be differences in the water content. Our current studies show that D_L is very sensitive to the water content, and a decrease from 30 wt % to 25 wt % water concentration results in a decrease in D_L by ~35% at 303 K. Above 30 wt % water, D_L changes very little (Filippov et al., to be published).

The temperature dependence of D_L in the l_d phase is found to follow the Arrhenius equation with apparent activation energies in the region of 33–36 kJ/mol (Fig. 5 C and Table 1). In the Arrhenius fits, shown as straight lines in the figure, the point at 298 K is excluded, since the close proximity to T_m influences D_L substantially. In the two-phase region the dependence is non-Arrhenius as one would expect, since D_L is the average value of D_L in two phases with different temperature dependence. The dotted lines represent D_L calculated from our diffusion data using the lever rule, and the phase borders determined by Almeida et al. (1992). It is clear that also for this system the experimental points in the two-phase area fit these lines. In the l_o phase the temperature dependence is again Arrhenius with an apparent activation energy of 55 kJ/mol. This is in good agreement with earlier published results in this temperature range on D_L of DMPC and a fluorinated CHOL analog (Orädd et al., 2002).

The DOPC/CHOL and POPC/CHOL systems

The facts that D_L:s of POPC and DOPC are a linear function of the CHOL content (Fig. 6) and that the reciprocal temperature dependence is linear at all temperatures with E_A:s in the range of 27–36 kJ/mol (Table 1) strongly suggest that the samples in these systems were all in the l_d phase. This can be understood by the low T_m for DOPC ($-20°$C) and POPC ($-3°$C). Both the experimental and theoretical phase diagrams show an upper critical temperature for the l_d-l_o coexistence region at $\sim$30–40°C above T_m, indicating that a possible two-phase region in the POPC and DOPC systems is located below the temperatures studied in this work. Further studies are presently being conducted at lower temperatures in order to find out whether a two-phase area can be detected also for these systems, as suggested by Thewalt and Bloom (1992).

CONCLUSIONS AND REMARKS

This work shows that it is possible to use the lipid lateral diffusion coefficients obtained by the pfg-NMR method to distinguish between the l_d and l_o phases in lipid-cholesterol systems. Differences in the concentration dependence and the apparent activation energies of the lipid diffusion between the two phases are clearly observed, especially for the SM/CHOL system. Although no new information on the phase borders could be obtained in the DMPC system, our data are in accordance with previously published phase studies. The different behavior in D_L for the two systems may be due to the difference in the hydrocarbon chain lengths for SM and DMPC. However, a conclusive interpretation will need further experiments for several phospholipids with different chain lengths, which are currently performed in our laboratory. For the POPC and DOPC systems it can be concluded that only the l_d phase is present at the temperatures studied.

In this study some important conclusions of possible biological relevance have been reached. There is a fast chemical exchange of lipids between l_o-domains floating around (rafts) in a sea of an l_d lipid bilayer (or vice versa). To obtain this fast exchange during the diffusion time of 100 ms the size of the domains is restricted to the order of μm or less. Moreover, the small but *nonzero* value of D_L in the l_o phase implies that an enzyme or protein attached to the cell membrane by, e.g., one or more hydrocarbon chains (as for the caveolins) can be easily incorporated into the domains of high molecular ordering and a high cholesterol content, where such proteins will be accumulated and subsequently activated.

REFERENCES

Almeida, P. F. F., W. L. C. Vaz, and T. E. Thompson. 1992. Lateral diffusion in the liquid phases of dimyristoylphosphatidylcholine/cholesterol bilayers: a free volume analysis. *Biochemistry*. 31:6739–6747.

Anderson, T. G., and H. M. McConnell. 2001. Condensed complexes and the calorimetry of cholesterol-phospholipid bilayers. *Biophys. J.* 81:2774–2785.

Brown, D. A. 1998. Structure and origin of ordered lipid domains in biological membranes. *J. Membr. Biol.* 164:103–114.

Callaghan, P. T. 1991. Principles of Nuclear Magnetic Resonance Microscopy. Clarendon, Oxford.

Chiu, S. W., E. Jakobsson, and H. L. Scott. 1999. Combined Monte-Carlo and molecular dynamics simulation of fully hydrated dioleoyl and palmitoyl-oleoyl phosphatidylcholine lipid bilayers. *Biophys. J.* 77:2462–2469.

De Kruijff, B., R. A. Demel, A. J. Slotboom, L. L. M. Van Deenen, and A. F. Rosenthal. 1973. The effect of the polar headgroup in the lipid-cholesterol interaction: a monolayer and differential scanning calorimetry study. *Biochim. Biophys. Acta*. 307:1–19.

Fiorini, R., E. Gratton, and G. Curatolo. 1989. Effect of cholesterol on membrane microheterogeneity: a study using 1,6-diphenyl-1,3,5-hexatriene fluorescence lifetime distributions. *Biochim. Biophys. Acta.* 1006:198–202.

Guo, W., V. Kurze, T. Huber, N. H. Afdahl, K. Beyer, and J. A. Hamilton. 2002. A solid-state NMR study of phospholipid-cholesterol interactions: sphingomyelin-cholesterol binary systems. *Biophys. J.* 83:1465–1478.

Haberkorn, R. A., R. G. Griffin, M. Meadows, and E. Oldfield. 1977. Deuterium nuclear magnetic resonance investigation of the dipalmitoyl lecithin-cholesterol-water system. *J. Am. Chem. Soc.* 99:7353–7355.

Ipsen, J. H., G. Kalström, O. G. Mouritsen, H. W. Wennerström, and M. J. Zuckermann. 1987. Phase equilibria in the phosphatidylcholine-cholesterol systems. *Biochim. Biophys. Acta*. 905:162–172.

Kärger, J., H. Pfeifer, and W. Heink. 1988. Principles and applications of self-diffusion measurements by nuclear magnetic resonance. *Advances in Magnetic Resonance*. 12:1–89.

Kuo, A.-L., and C. G. Wade. 1979. Lipid lateral diffusion by pulsed nuclear magnetic resonance. *Biochemistry*. 18:2300–2308.

Ladha, S., A. R. Mackie, L. J. Harvey, D. C. Clark, E. J. A. Lea, M. Brullemans, and H. Duclohier. 1996. Lateral diffusion in planar lipid bilayers: a fluorescence recovery after photobleaching investigation of its modulation by lipid composition, cholesterol, or alamethicin content and divalent cations. *Biophys. J.* 71:1364–1373.

Leathes, J. B. 1925. Role of fats in vital phenomena. *Lancet.* 208:853–856.

Lemmich, J., K. Mortensen, J. H. Ipsen, T. Honger, R. Bauer, and O. G. Mouritsen. 1997. The effect of cholesterol in small amount on lipid-bilayer softness in the region of the main phase transition. *Eur. Biophys. J.* 25:293–304.

Lindblom, G., L. B.-Å. Johansson, and G. Arvidson.1981. Effect of cholesterol in membranes. Pulsed nuclear magnetic resonance measurements of lipid lateral diffusion. *Biochemistry.* 20:2204–2207.

Lindblom, G., and G. Orädd. 1994. NMR studies of translational diffusion in lyotropic liquid crystals and lipid membranes. *Prog. Nucl. Magn. Reson. Spectrosc.* 26:483–515.

Maulik, P. R., and G. G. Shipley. 1996a. Interactions of N-stearoyl sphingomyelin with cholesterol and dipalmitoyl phosphatidylcholine in bilayer membranes. *Biophys. J.* 70:2256–2265.

Maulik, P. R., and G. G. Shipley. 1996b. N-palmitoyl sphingomyelin bilayers: structure and interactions with cholesterol and dipalmitoyl-phosphatidylcholine. *Biochemistry.* 35:8025–8034.

McIntosh, T. J. 1978. The effect of cholesterol on the structure of phosphatidylcholine bilayers. *Biochim. Biophys. Acta.* 513:43–58.

Oldfield, E., M. Meadows, D. Rice, and R. Jacobs. 1978. Spectroscopic studies of specifically deuterium labeled membrane systems. Nuclear magnetic resonance investigation of the effects of cholesterol in model systems. *Biochemistry.* 17:2727–2740.

Orädd, G., G. Lindblom, and P. W. Westerman. 2002. Lateral diffusion of cholesterol and DMPC in a lipid bilayer measured by pfg-NMR. *Biophys. J.* 83:2702–2704.

Polson, J. M., I. Vattulainen, H. Zhu, and M. J. Zuckermann. 2001. Simulation study of lateral diffusion in lipid-sterol bilayer mixtures. *European Physical Journal E.* 5:485–497.

Radhakrishnan, A., X.-M. Li, R. E. Brown, and H. M. McConnell. 2001. Stoichiometry of cholesterol- sphingomyelin condensed complexes in monolayers. *Biochim. Biophys. Acta.* 1511:1–6.

Radhakrishnan, A., and H. M. McConnell. 1999. Condensed complexes of cholesterol and phospholipids. *Biophys. J.* 77:1507–1517.

Rietveld, A., and K. Simons. 1998. The differential miscibility of lipids as the basis for the formation of functional membrane rafts. *Biochim. Biophys. Acta.* 1376:467–479.

Samsonov, A. V., I. Mihalyov, and F. S. Cohen. 2001. Characterization of cholesterol-sphingomyelin domains and their dynamics in bilayer membranes. *Biophys. J.* 81:1486–1500.

Sankaram, M. B., and T. E. Thompson. 1990. Interaction of cholesterol with various glycerophospholipids and sphingomyelin. *Biochemistry.* 29:10670–10675.

Simons, K., and E. Ikonen. 1997. Functional rafts in cell membranes. *Nature.* 387:569–572.

Smaby, J. M., H. L. Brockman, and R. E. Brown. 1994. Cholesterol's interfacial interactions with sphingomyelins and phosphatidylcholines: hydrocarbon chain structure determines the magnitude of condensation. *Biochemistry.* 33:9135–9142.

Smondyrev, A. M., and M. L. Berkowitz. 1999. Structure of dipalmitoyl-phosphatidylcholine/cholesterol bilayer at low and high cholesterol concentrations: molecular dynamic simulation. *Biophys. J.* 77:2075–2089.

Stockton, G. W., and I. C. P. Smith. 1976. A deuterium NMR study of the condensing effect of cholesterol on egg phosphatidylcholine bilayer membranes. I. Perdeuterated fatty acid probes. *Chem. Phys. Lipids.* 17:251–263.

Tanner, J. E. 1970. Use of the stimulated echo in NMR diffusion studies. *J. Chem. Phys.* 52:2523–2526.

Thewalt, J. L., and M. Bloom. 1992. Phosphatidylcholine: cholesterol phase diagrams. *Biophys. J.* 63:1176–1181.

Trouard, T. P., A. A. Nevzorov, T. M. Alam, C. Job, J. Zajicek, and M. F. Brown. 1999. Influence of cholesterol on dynamics of dimyristoylphosphatidylcholine bilayers as studied by deuterium NMR relaxation. *J. Chem. Phys.* 110:8802–8818.

Ulmius, J., H. W. Wennerström, G. Lindblom, and G. Arvidson. 1975. Proton NMR bandshape studies of lamellar liquid crystals and gel phases containing lecithins and cholesterol. *Biochim. Biophys. Acta.* 389:197–202.

Vaz, W. L. C., R. M. Clegg, and D. Hallman. 1985. Translational diffusion of lipids in liquid crystalline phases phosphatidylcholine multibilayers. A comparison of experiment with theory. *Biochemistry.* 24:781–786.

Vist, M. R., and J. H. Davis. 1990. Phase equilibria of cholesterol/dipalmitoylphosphatidylcholine mixtures: ^{2}H nuclear magnetic resonance and differential scanning calorimetry. *Biochemistry.* 29:451–464.

Wassall, S. R. 1996. Pulsed field gradient-spin echo NMR studies of water diffusion in a phospholipid model membrane. *Biophys. J.* 71:2724–2732.

Wästerby, P., G. Orädd, and G. Lindblom. 2002. Anisotropic water diffusion in macroscopically oriented lipid bilayers studied by pulsed magnetic field gradient NMR. *J. Magn. Reson.* 157:156–159.

Weisz, K., G. Gröbner, C. Mayer, J. Stohrer, and G. Kothe. 1992. Deuteron nuclear magnetic resonance study of the dynamic organization of phospholipid/cholesterol bilayer membranes: molecular properties and viscoelastic behavior. *Biochemistry.* 31:1100–1112.

Yeagle, P. L. 1985. Cholesterol and the cell membrane. *Biochim. Biophys. Acta.* 822:267–287.